ChemComm

Accepted Manuscript

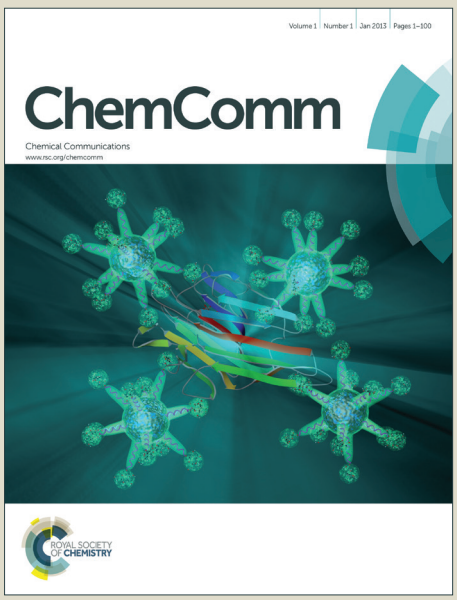

ROYAL SOCIETY OF CHEMISTRY

www.rsc.org/chemcomm

Journal Name

RSCPublishing

COMMUNICATION

Excited-state electronic couplings in 1,3-butadiyne-bridged Zn(II)porphyrin dimer and trimer

Cite this: DOI: 10.1039/xoxxoooooox

Received ooth January 2012,
Accepted ooth January 2012

DOI: 10.1039/xoxxoooooox

www.rsc.org/

Sangsu Lee,[a] Heejae Chung,[a] Sumito Tokuji,[b] Hideki Yorimitsu,[b] Atsuhiro Osuka*[b] and Dongho Kim*[a]

Electronic couplings in 1,3-butadiyne-bridged Zn(II) porphyrin dimer D and trimer T have been probed by measurements of their excited-state properties at ensemble and single molecular levels. While single chromophore-like, strongly interacting behaviors are revealed for D, the coupling in T is indicated to be not so strong.

Recently, many research groups have made strenuous efforts toward the development of π-conjugated molecular systems, which may be utilized as functional soft materials and molecular-level devices for advanced technological functions. In particular, conjugated porphyrin oligomers have been one of the most extensively studied molecular motifs in light of their high stabilities, strong electronic absorptions in the visible region, emissive properties of certain porphyrins, efficient energy and electron transfer reactions, nonlinear optical properties, and easily tunable optical properties.[1] To improve these properties or explore novel functions of porphyrin oligomers, it is vital to understand the electronic interactions among the porphyrin components. Factors such as orientation, distance, and connecting bridge are considered to play important roles in achieving effective electronic communication.

In this context, we chose *β*-to-*β* 1,3-butadiyne-bridged cyclic diporphyrin **D** and triporphyrin **T**[2] and comparatively investigated their optical properties (Scheme 1). *meso*-to-*meso* 1,3-Butadiyne-bridged porphyrin oligomers have been extensively studied as more strongly coupled systems[3] and gigantic cyclic porphyrin arrays have been explored recently.[3c] In the present case, the porphyrin moieties are bridged by two 1,3-butadiyne bridges via *β*-to-*β* connection to form a rectangular and a triangular shape for **D** and **T**,[4] respectively, plausibly with different strain at the bridges.

The absorption and fluorescence spectra of **D** and **T** were recorded in toluene at room temperature (Fig. 1). As compared to the absorption features of ZnTPP monomer **M**, noticeable red-shifts were observed in **D** and **T** as a consequence of extended π-conjugation through the 1,3-butadiyne bridges. The blue-shift in the fluorescence spectrum of **T** may be ascribed to its less effective π-conjugation as compared with that of **D**, probably due to its slightly

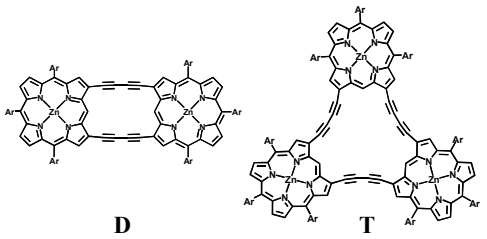

Scheme 1 Structures of **D** and **T**; Ar = 3,5-di-*tert*-butylphenyl.

distorted 1,3-butadiyne structure.[2] Moreover, the B-band became split into two bands, from which the splitting energies were estimated to be 2755 and 1709 cm^{-1} for **D** and **T**, respectively. Though **D** and **T** have almost planar structure which can lead to a strong dipole-dipole interaction, the through-space dipole-dipole interaction between the porphyrin moieties should be weaker than the previously studied directly linked porphyrin arrays because of longer center-to-center distances. But the splitting energies of **D** and **T** are similar to those of directly linked porphyrin arrays,[5] which is

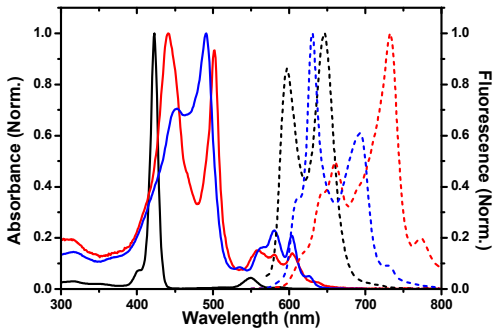

Fig. 1 Steady-state absorption (solid lines) and fluorescence spectra (dotted lines) of **M** (black), **D** (red), **T** (blue) in toluene. The fluorescence spectra were obtained with photoexcitation at 420 (**M**), 441 (**D**) and 491 nm (**T**), respectively.

induced by the butadiyne bridges. Furthermore, radiative, nonradiative rate constants and fluorescence quantum yields of **D** and **T** are different from those of **M** (Table S1 in the SI). Additionally, the fluorescence lifetimes of **D** and **T** were measured to be 2.37 and 2.09 ns by time-correlated single photon counting (TCSPC) technique, which are slightly longer than that of **M** (1.99 ns) (Fig. S1 in the SI). In previous study, we could confirm that the fluorescence lifetimes gradually decrease as the number of porphyrin units increases in the arrays.[5] But the fluorescence lifetimes of **D** and **T** are longer than that of **M**. These differences infer that the optical properties of the lowest Q-state might differ from those of **M**.

Fluorescence excitation anisotropy measurements provide useful information on the nature of the electronic states, such as the orientation of the transition dipole moments of the absorbing state with respect to that of the monitored emissive state. Fluorescence excitation anisotropy spectra were monitored at the highest fluorescence peaks (Fig. S2 in the SI). In the case of **M**, the overall spectrum exhibited extremely weak signals because of an ultrafast depolarization of excited state due to degenerate transient dipoles in both B- and Q-states as well as an efficient depolarization via fast rotational reorientation processes.[6] On the other hand, **D** and **T** have larger hydrodynamic volumes than **M**, and their rotational diffusion times were found to be slower than that of **M** (Fig. S3 in the SI). As a result of the slow depolarization, we observed larger anisotropy values of **D** and **T** compared to that of **M**. But, **D** and **T** show unusual behaviors in the steady-state fluorescence excitation anisotropy. Unlike *meso-meso* linked porphyrin oligomers,[1e,5] **D** and **T** show positive anisotropy values in the entire absorption region, indicating that the transition dipoles of the two B-states and lowest emissive Q-state should be parallel. From these results, we can assume that a new electronic excited state is generated by strong electronic coupling through the butadiyne linkers.

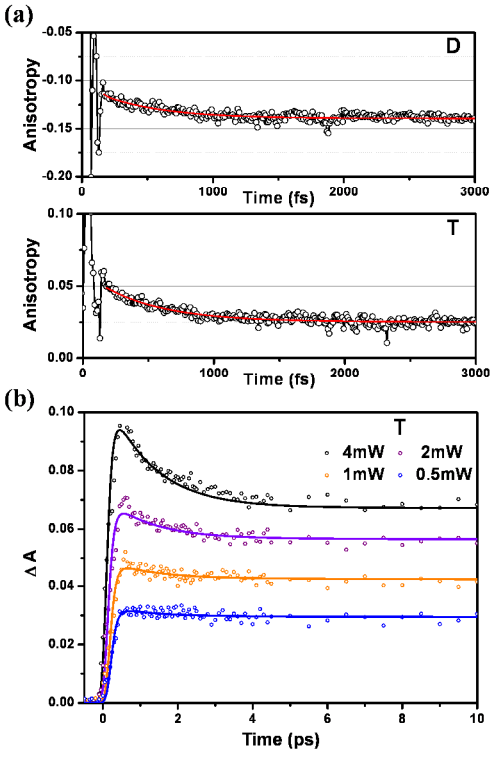

Fig. 2 (a) Transient absorption anisotropy (TAA) decay profiles of **D** (top), **T** (bottom) in toluene by photoexcitation around 610 nm and probed at 530 nm. (b) Pump-power dependent transient absorption decay profiles of **T** in toluene with photoexcitation at 460 nm and probed at 655 nm.

To explore the new excited-state dynamics, we have measured transient absorption anisotropy (TAA) decay and pump-power dependence on transient absorption (TA) decay. In general, stimulated emission (SE) or ground-state bleaching (GSB) signal gives simpler kinetic information rather than excited-state absorption (ESA), because only two states are enough to describe the population decay mechanism. Unfortunately, due to interferences by the broad and intense induced absorption signal in the whole visible region in our samples, the SE and GSB signals of the Q-state could not be detected exclusively (Fig. S4 in the SI). Therefore, we chose the ESA signal at 530 nm as a probe, which corresponds to the excited-state absorption of the Q-state upon photoexcitation at 610 nm (Fig. 2(a)). As a reference for an analysis of TAA decay in **D** and **T**, we carried out time-resolved anisotropy decay measurements of **M** (Fig. S5 and Table S2 in the SI).[7] We chose the excited-state absorption (ESA) signal at 500 nm as a probe, which corresponds to the excited-state absorption of the Q-state after photoexcitation at 550 nm. In this experiment, we could confirm that the infinite anisotropy value is 0.06 after vibrational relaxation and internal conversion from the B- to Q-state (Table S2 in the SI). On the other hand, the anisotropy of **T** slowly decayed from the initial anisotropy value of 0.06 with the time constant of 470 fs (Fig. 2(a) and Table S2 in the SI). The initial anisotropy value of **T** is presumably contributed by the intrinsic electronic dephasing of the congested Q-states within the monomer in **T** because it coincides with the infinite value of **M** at the Q-state. Furthermore, the infinite anisotropy value of **T** coincided with the initial anisotropy value of **T** found in the TCSPC measurement (Fig S3 in the SI). Accordingly, the subsequent anisotropy decay processes with the time constant of 470 fs of **T** should be a consequence of an excitation energy hopping (EEH) process. From the observed anisotropy depolarization time of 470 fs, we could evaluate the EEH time of 1.4 ps based on a polygon model detailed in previous work.[8] Importantly, the time-resolved anisotropy decay profile of **D** is quite different from that of **T**. The anisotropy value is increased to more negative value starting from -0.11 with the time constant of 460 fs (Fig. 2(a) and Table S2 in the SI). Since the anisotropy value is sensitive to the change in the orientation of transition dipole moments, we can infer that the observed anisotropy rise dynamics comes from two non-degenerate Q-states of **D**. Because the two adjacent porphyrin moieties of **D** are bridged by two butadiyne linkers, their relative orientation is rather planar compared with other porphyrin dimers and hence, the π-conjugation extends to the whole molecule. Therefore, degenerate Q-states of **M** become two non-degenerate Q-states of **D** with two orthogonally orientated transition dipoles. Accordingly, the internal conversion process between these orthogonally oriented Q-states in **D** leads to a negative increase of absolute anisotropy value of **D**.

Pump-power dependent TA measurement is a strong indication of S_1-S_1 exciton-exciton annihilation, because intense excitation or photons of high density may generate two or more excitons in the multichromophoric array and the recombination between excitons gives rise to a fast deactivation channel. When the pump power is increased in **T**, the contribution by the relatively fast τ_1 (1.2 ps) component is enhanced, as compared to the slowest τ_2 (2100 ps) component (Fig 2(b) and Table S3 in the SI). From the observed exciton-exciton annihilation time of 1.2 ps, we retrieved the EEH time of 3.6 ps from the polygon model.[8] The average of the two different experimental observables, anisotropy depolarization and exciton-exciton annihilation times gives rise to the EEH time of ~2.5 ps. To reveal the underlying mechanism for the EEH processes in **T**, we calculated the Förster-type resonance energy transfer (FRET) time for **T**, which was estimated to be 64 ps (Table S4 in the SI).[9] From a large discrepancy between the observed EEH time and the calculated FRET time (2.5 vs. 64 ps), we can assume that the EEH

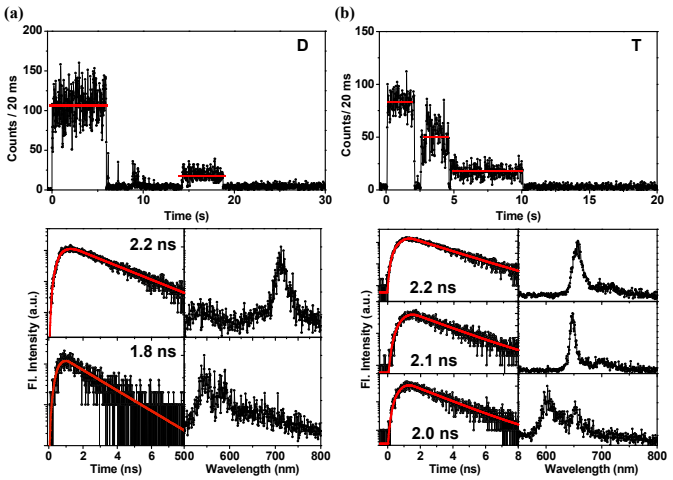

Fig. 3 Representative fluorescence intensity trajectories (FITs) and corresponding spectra of (a) **D** and (b) **T**.

processes in **T** are largely mediated by the through-bond interactions. Meanwhile, **D** displayed no power dependence on the TA decay with only a slow decay component that matches the S_1 state lifetime found in the TCSPC measurement (Fig. S4 in the SI).

To investigate the electronic coupling dynamics in **D** and **T** at the single molecule level, we have simultaneously measured the single-molecule fluorescence intensity trajectories (FITs), fluorescence lifetimes and fluorescence spectra (Fig. 3). The fluorescence spectra were obtained at each FIT level, whose spectral features at the first emissive level are similar to those observed in solution. Furthermore, the fluorescence lifetime of **D** at the first-step is longer than that of **T**, which is in agreement with the ensemble-level results and we found that more than 70% of both molecules exhibit the collective one-step photobleaching behaviors in the statistical analysis (Fig. S6 in the SI). From these features, we can conclude that **D** and **T** at the first emissive levels are strongly conjugated through the 1,3-butadiyne bridges. The slightly higher probability of **D** to show one-step photobleaching process in FITs compared with **T** also suggests that the porphyrin moieties in **D** are more strongly coupled. Moreover, in the case of **D**, we could observe that 23% of the total probed molecules showed two-step FITs. On the other hand, for **T**, 24% showed two-step FITs and 5% showed three-step FITs (Fig. S7 in the SI). These stepwise photobleaching behaviors in the FITs of **D** and **T** are attributable to the conformational heterogeneities imposed by the nanoenviroments in host PMMA matrix. To obtain detailed information on the stepwise photobleaching behaviors, we have monitored the fluorescence spectra at each FIT step. After one step photobleaching in **D**, the fluorescence spectra were blue-shifted to resemble the fluorescence spectral features of **M**, indicating that the remaining porphyrin moiety behaves as an individual porphyrin entity. In a similar manner, the fluorescence spectra of **T** after one-step photobleaching showed spectral features that are similar to those of partially conjugated dimer. Finally, after two-step photobleaching, the fluorescence spectra were further blue-shifted to resemble that of **M**. Accordingly, the spectroscopic features, fluorescence lifetimes as well as FITs at the single molecule level are in good accordance with the molecular structures of **D** and **T**.

In order to gain further insight into the electronic couplings in **D** and **T**, quantum chemical approaches were introduced such as molecular orbital (MO) analysis at the B3LYP/6-31G(d) level using the optimized structures (Fig. S8 in the SI). Eight representative frontier MOs were calculated with similar energies for **D** and **T**. Interestingly, the electron densities of the frontier MOs of **D** and **T** are slightly different from each other. While the overall electron densities were fully delocalized over the two porphyrin moieties and 1,3-butadiyne bridges for **D**, partially concentrated electron densities were observed on the three porphyrin subunits for **T**.

Overall, in this study, we could clarify the manner of electronic communication through π-conjugated linkers in the two representative dimer and trimer systems. Our experimental and theoretical results suggest that **D** can be regarded as single chromophore owing to the strong coupling through the 1,3-butadiyne bridges and **T** as a partially coupled system because of its slightly distorted structure and weaker dipole-dipole interaction than that of **D** due to its triangular shape.

The work at Yonsei University was financially supported by the Mid-career Researcher program (2005-0093839) and Global Research Laboratory (2013K1A1A2A02050183) administered through the National Research Foundation of Korea (NRF) funded by the Ministry of Education, Science and Technology (MEST). The quantum calculations were performed using the supercomputing resources of the Korea Institute of Science and Technology Information (KISTI). The work at Kyoto was supported by Grants-in-Aid (No. 25220802 (S)) for Scientific Research from MEXT. S. T. thanks JSPS fellowship for Young Scientists.

Notes and references

[a]*Department of Chemistry, Yonsei University, Seoul 120-749, Korea. E-mail: dongho@yonsei.ac.kr; Tel: +82 2-2123-2652*
[b]*Department of Chemistry and Graduate School of Science, Kyoto University, Sakyo-ku, Kyoto 606-8502, Japan. E-mail: osuka@kuchem.kyoto-u.ac.jp; Tel: +81 75-753-4008*

† Electronic Supplementary Information (ESI) available: [details of any supplementary information available should be included here]. See DOI: 10.1039/c000000x/

1 (a) M. R. Wasielewski, *Chem. Rev.,* 1992, **92**, 435; (b) D. Gust, T. A. Moore and A. L. Moore, *Acc. Chem. Res*., 2001, **34**, 40; (c) D. Holten, D. F. Bocian and J. S. Lindsey, *Acc. Chem. Res*., 2002, **35**, 57; (d) M. Iyoda, J. Yamakawa and M. J. Rahman, *Angew. Chem. Int. Ed*., 2011, **50**, 10522; (e) D. Kim and A. Osuka, *Acc. Chem. Res*., 2004, **37**, 735; (f) N. Aratani, D. Kim and A. Osuka, *Acc. Chem. Res*., 2009, **42**, 1922.
2 S. Tokuji, H. Yorimitsu and A. Osuka, *Angew. Chem. Int. Ed*., 2012, **51**, 12357.
3 (a) H. L. Anderson, *Inorg. Chem.,* 1994, **33**, 972; (b) P. N. Taylor and H. L. Anderson, *J. Am. Chem. Soc*., 1999, **121**, 11538; (c) M. Hoffmann, C. J. Wilson, B. Odell and H. L. Anderson, *Angew. Chem. Int. Ed*., 2007, **46**, 3122.
4 (a) V. S.-Y. Lin, S. G. DiMagno and M. J. Therien, *Science*, 1994, **264**, 1105; (b) J. J. Gosper and M. Ali, *J. Chem. Soc.,Chem. Commun.*, 1994, 1707; (c) B. König and H. Zieg, *Synthesis*, 1998, 171.
5 Y. H. Kim, D. H. Jeong, D. Kim, S. C. Jeoung, H. S. Cho, S. K. Kim, N. Aratani and A. Osuka, *J. Am. Chem. Soc*., 2001, **123**, 76.
6 H.-Z. Yu, J. S. Baskin and A. H. Zewail, *J. Phys. Chem., A*, 2002, **106**, 9845.
7 M.-C. Yoon, S. Lee, S. Tokuji, H. Yorimitsu, A. Osuka and D. Kim, *Chem. Sci.*, 2013, **4**, 1756.
8 S. E. Bradforth, R. Jimenez, F. van Mourik, R. van Grondelle and G. R. Fleming, *J. Phys. Chem.*, 1995, **99**, 16179.
9 Z. S. Yoon, M.-C. Yoon and D. Kim, *J. Photochem. Photobiol., C*, 2005, **6**, 249.